

Mo/Rh Carboxylate: Heterometallic Compound Built of Homometallic Paddlewheel Units

Bo Li,[†] Haitao Zhang,[†] Lan Huynh,[†] Mikhael Shatruk,^{‡§} and Evgeny V. Dikarev^{*†}

Department of Chemistry, University at Albany, Albany, New York 12222, and Department of Chemistry, Texas A&M University, College Station, Texas 77842

Received May 9, 2007

Mixed-metal molybdenum(II)/rhodium(II) tetra(trifluoroacetate) of the composition $[(\text{MoRh})(\text{O}_2\text{CCF}_3)_4]$ has been obtained from the gas-phase reaction between volatile carboxylates, $[\text{Mo}_2(\text{O}_2\text{CCF}_3)_4]$ and $[\text{Rh}_2(\text{O}_2\text{CCF}_3)_4]$. This is an interesting system for which a single-crystal X-ray investigation fails to provide an unambiguous evidence of whether the product consists of the initial homometallic or newly formed heterometallic paddlewheel units. In the solid-state structure both metal atoms occupy the same crystallographic position, while the M–M and M–O distances are averaged with respect to the parent homometallic compounds. Nevertheless, the results of mass-spectrometric and magnetic measurements clearly indicate that the title bimetallic carboxylate contains a statistical mixture of homometallic dimolybdenum and dirhodium units. The product can be considered as a result of cocrystallization of isomorphous paddlewheel molecules.

Introduction

Since the report of correct structure for dimolybdenum tetraacetate,¹ numerous paddlewheel carboxylates have been synthesized and characterized,^{2,3} with the vast majority of them being homonuclear species. Examples of heterobimetallic compounds are limited to quadruple-bonded Group VI transition metal carboxylates, $[(\text{MoM})(\text{O}_2\text{CR})_4]$ (M = Cr, R = Me;⁴ M = W, R = ^tBu⁵) and several dinuclear molecules without metal–metal bonding.⁶ Although the controlled synthesis of heterobimetallic complexes represents a significant challenge, it is a very attractive idea to create a dinuclear

molecule with distinctly different properties at two potential metal binding sites (e.g., strong–weak Lewis acids or Lewis acid–base pair).⁷ For example, an interesting synergistic effect is observed when certain heterometallic catalysts show better performance compared to their homometallic counterparts.⁸ In general, the assembly of heterometallic paddlewheel carboxylates in the solid state can occur in two different ways: (i) through formation of a “true” heterobi-

* To whom correspondence should be addressed. Phone: (518) 442-4401. Fax: (518) 442-3462. E-mail: dikarev@albany.edu.

[†] University at Albany.

[‡] Texas A&M University.

[§] Present address: Department of Chemistry and Biochemistry, Florida State University, Tallahassee, FL 32306

(1) Lawton, D.; Mason, R. *J. Am. Chem. Soc.* **1965**, *87*, 921.

(2) (a) Cotton, F. A.; Murillo, C. A.; Walton, R. A. *Multiple Bonds Between Metal Atoms*, 3rd ed.; Springer Science and Business Media Inc.: New York, 2005.

(3) (a) Campbell, G. C.; Haw, J. F. *Inorg. Chem.* **1988**, *27*, 3706. (b) Allman, T.; Goel, R. C.; Jha, N. K.; Beauchamp, A. L. *Inorg. Chem.* **1984**, *23*, 914. (c) Lau, W.; Huffman, J. C.; Kochi, J. K. *J. Am. Chem. Soc.* **1982**, *104*, 5515. (d) Wojtczak, W. A.; Hampden-Smith, M. J.; Duesler, E. N. *Inorg. Chem.* **1998**, *37*, 1781. (e) Yang, K.-C.; Chang, C.-C.; Yeh, C.-S.; Lee, G.-H.; Peng, S.-M. *Organometallics* **2001**, *20*, 126. (f) Frank, W.; Reiland, V.; Reiss, G. J. *Angew. Chem., Int. Ed. Engl.* **1998**, *37*, 2984. (g) Dikarev, E. V.; Li, B. *Inorg. Chem.* **2004**, *43*, 3461.

(4) Garner, C. D.; Senior, R. G.; King, T. J. *J. Am. Chem. Soc.* **1976**, *98*, 3526.

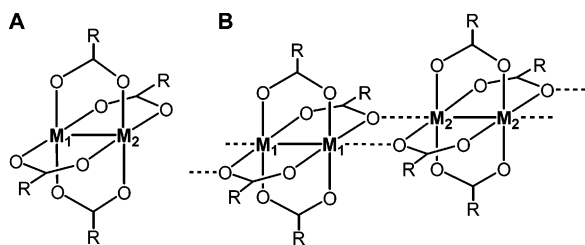
(5) (a) Katovic, V.; Templeton, J. L.; Hoxmeier, R. J.; McCarley, R. E. *J. Am. Chem. Soc.* **1975**, *97*, 5300. (b) Katovic, V.; McCarley, R. E. *J. Am. Chem. Soc.* **1978**, *100*, 5586. (c) Chisholm, M. H.; D'Acchioli, J. S.; Pate, B. D.; Patmore, N. J.; Dalal, N. S.; Zipse, D. *J. Inorg. Chem.* **2005**, *44*, 1061.

(6) (a) Smith, G.; O'Reilly, E. J.; Kennard, C. H. L.; White, A. H. *J. Chem. Soc., Dalton Trans.* **1985**, 243. (b) Yang, Y.-Y.; Wu, Y.-L.; Long, L.-Sh.; Chen, X.-M. *J. Chem. Soc., Dalton Trans.* **1999**, 2005. (c) Calvo-Perez, V.; Shang, M.; Yap, G. P. A.; Rheingold, A. L.; Fehlner, T. P. *Polyhedron* **1999**, *18*, 1869. (d) Wang, X.; Jin, T.; Jin, Q.; Xu, G.; Zhang, S. *Polyhedron* **1994**, *13*, 2333. (e) Gao, F.; Wang, R.-Y.; Jin, T.-Zh.; Xu, G.-X.; Zhou, Zh.-Y.; Zhou, X.-G. *Polyhedron* **1997**, *16*, 1357. (f) Balch, A. L.; Davis, B. J.; Fung, E. Y.; Olmstead, M. M. *Inorg. Chim. Acta* **1993**, *212*, 149. (g) He, F.; Tong, M.-L.; Yu, X.-L.; Chen, X.-M. *Inorg. Chem.* **2005**, *44*, 559. (h) Yang, Y.-Y.; Chen, X.-M.; Ng, S. W. *Aust. J. Chem.* **1999**, *52*, 983. (i) Adam, S.; Bauer, A.; Timpe, O.; Wild, U.; Mestl, G.; Bensch, W.; Schlögl, R. *Chem.–Eur. J.* **1998**, *4*, 1458.

(7) (a) Shibasaki, M.; Yoshikawa, N. *Chem. Rev.* **2002**, *102*, 2187. (b) Shibasaki, M.; Kanai, M.; Funabashi, K. *Chem. Commun.* **2002**, 1989. (c) Steinhagen, H.; Helmchen, G. *Angew. Chem., Int. Ed. Engl.* **1996**, *35*, 2339. (d) Rowlands, G. J. *Tetrahedron* **2001**, *57*, 1865.

(8) (a) Wheatley, N.; Klack, P. *Chem. Rev.* **1999**, *99*, 3379. (b) Yamagiwa, N.; Qin, H.; Matsunaga, S.; Shibasaki, M. *J. Am. Chem. Soc.* **2005**, *127*, 13419.

Scheme 1



metallic unit bridged by carboxylate ligands and further supported by direct metal–metal bonding (Scheme 1, **A**), providing homogenization at the molecular level, and (ii) through Lewis acid–base adduct formation (**B**) giving an ordered or statistical arrangement of homonuclear units in infinite chains. To this end, we have recently reported that bismuth(II) trifluoroacetate^{3g} acts as a metalloligand toward transition metal ($M = \text{Rh}, \text{Ru}$) fragments affording remarkable heterobimetallic molecules, which adopt the paddlewheel structure **A**.⁹ Herein we communicate the synthesis, structure, and characterization of new heterometallic molybdenum(II)/rhodium(II) tetra(trifluoroacetate) (**1**), that conforms to the type **B** with statistical distribution of homonuclear units in the solid-state structure.

Results and Discussion

Molybdenum/rhodium trifluoroacetate (**1**) has been obtained in the form of single crystals from the solid-state reaction by heating the mixture of unsolvated $[\text{Rh}_2(\text{O}_2\text{CCF}_3)_4]$ and $[\text{Mo}_2(\text{O}_2\text{CCF}_3)_4]$ at 150 °C in a sealed ampule. While the green color of **1** appeared to be just a bit lighter than that of the starting dirhodium tetracarboxylate, the new complex exhibits noticeably greater stability toward moist air. Compound **1** is soluble in anhydrous, deoxygenated toluene, acetone, ether, ethyl alcohol, and THF, while only partially soluble in non-coordinating CHCl_3 and CH_2Cl_2 .

Elemental analysis for the crystalline sample of **1** gave a Mo/Rh metal ratio of close to 1:1. An X-ray diffraction study of the single crystals revealed that compound crystallizes in triclinic space group with unit cell parameters similar to those of both homometallic carboxylates (Table 1) that are, in fact, isomorphous. Crystallographically this means that there is one bimetallic molecule in the unit cell. The structure was initially solved in noncentrosymmetric space group $P1$ with two crystallographically independent metal positions assigned to molybdenum and rhodium. However, the geometry around each position appeared essentially the same, while thermal parameters were substantially different (0.024 and 0.036, respectively). In addition, the value of Flack parameter was close to $x = 0.5$. The structure of **1** was finally refined in centrosymmetric space group $P\bar{1}$ with one crystallographically independent metal position constrained as 50% Mo and 50% Rh, according to the results of elemental analysis. No disorder at the metal or oxygen sites was detected. As

Table 1. Selected Structural Parameters, Bond Distances (Å) and Angles (deg) for **1** and Its Parent Homometallic Carboxylates, $[\text{M}_2(\text{O}_2\text{CCF}_3)_4]$ ($M = \text{Mo}, \text{Rh}$)

	$[\text{Mo}_2]$	$[\text{Rh}_2]^{(10)}$	1
cryst syst	triclinic	triclinic	triclinic
space group	$P\bar{1}$	$P\bar{1}$	$P\bar{1}$
a (Å)	5.5662(8)	5.2499(5)	5.3385(5)
b (Å)	8.2207(12)	8.491(2)	8.4547(8)
c (Å)	8.9579(13)	9.172(2)	9.1418(8)
α (deg)	87.515(2)	88.80(1)	89.6540(10)
β (deg)	85.862(2)	88.53(1)	89.6720(10)
γ (deg)	80.617(2)	76.43(1)	77.0450(10)
V (Å ³)	403.15(10)	397.3(1)	402.11(6)
Z	1	1	1
M–M	2.1036(4)	2.3813(8)	2.2888(5)
M–O	2.115(2)	2.047(4)	2.060(3)
M...O	2.678(3)	2.337(4)	2.439(3)
M–M–O	91.76(5)	88.2(1)	89.42(7)
M–M...O	158.33(6)	169.3(1)	166.44(6)

Table 2. Selected Bond Distances (Å) for **2** and the THF Bisadducts of Homometallic Carboxylates

	$[\text{Mo}_2]$	$[\text{Rh}_2]$	2
M–M	2.1202(5)	2.4074(8)	2.3186(8)
M–O	2.121(2)	2.039(3)	2.063(3)
M...O _{THF}	2.478(3)	2.260(4)	2.318(3)

Table 3. Spectroscopic Characterization of Compound **1** and Parent Homometallic Carboxylates, $\text{M}_2(\text{O}_2\text{CCF}_3)_4$ ($M = \text{Mo}, \text{Rh}$)

	$[\text{Mo}_2]$	$[\text{Rh}_2]$	1
¹⁹ F NMR (C_7D_8), δ	–71.49	–73.98	–71.50, –73.95
IR (KBr, cm^{-1}): $\nu_{\text{asym}}(\text{CO})$	1594s	1647s	1593s, 1655s
$\nu_{\text{sym}}(\text{CO})$	1455 m	1465 m	1458 m
UV–vis (C_7H_8), λ_{max} , nm	304, 315(sh)	312, 356	310, 352

expected, the crystal structure is similar to those of the parent Mo^{II} and Rh^{II} trifluoroacetates. The major structural element is a paddlewheel unit (Figure 1, left) with a metal–metal bond distance of 2.2888(5) Å that falls between the Mo–Mo and Rh–Rh bond lengths in corresponding homometallic carboxylates (Table 1). The same trend is also observed for other bond lengths and angles in the structure of **1**. The paddlewheel molecules are combined into 1D infinite chains (Figure 1, right) through axial $\text{M}\cdots\text{O}$ interactions (2.439(3) Å) that are also between those for the molybdenum and rhodium trifluoroacetates.

This is an interesting system for which the single-crystal X-ray study clearly fails to provide an unambiguous evidence of whether the product consists of starting homometallic (Scheme 1, **B**) or newly formed heterometallic paddlewheel units (Scheme 1, **A**). The previously reported structures of the heterometallic molecules $[(\text{MoM})(\text{O}_2\text{CR})_4]$ ($M = \text{Cr}, \text{W}$)^{4,5} exhibit the same problem, and other methods have been employed to prove a “true” heterobimetallic character of these compounds. For instance, the iodine–acetonitrile bisadduct of the Mo–Cr molecule was found to have two ordered metal sites in the crystal structure.

Thus, we have decided to prepare a discrete bimetallic complex by dissolution of the crystals of **1** in THF. Our expectations were based on the fact that dimolybdenum and dirhodium complexes display very different axial distances to the oxygen atom of THF (Table 2). Indeed, pale-violet crystals of a tetrahydrofuran bisadduct, $[(\text{MoRh})(\text{O}_2\text{CCF}_3)_4](\text{THF})_2$ (**2**), were harvested from the solution. Unfortunately,

(9) (a) Dikarev, E. V.; Gray, T. G.; Li, B. *Angew. Chem., Int. Ed.* **2005**, *44*, 1721. (b) Dikarev, E. V.; Li, B.; Zhang, H. *J. Am. Chem. Soc.* **2006**, *128*, 2814.

(10) Cotton, F. A.; Dikarev, E. V.; Feng, X. *Inorg. Chim. Acta* **1995**, *237*, 19.

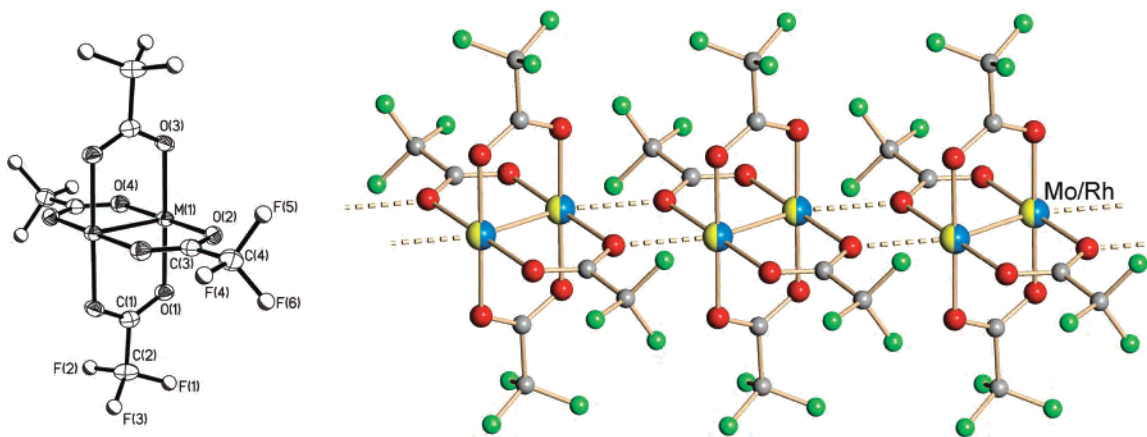


Figure 1. ORTEP view (50% probability thermal ellipsoids) of the paddlewheel molecule in the structure of heterobimetallic Mo/Rh trifluoroacetate (left). A fragment of a 1D polymeric chain built on intermolecular interactions in **1**.

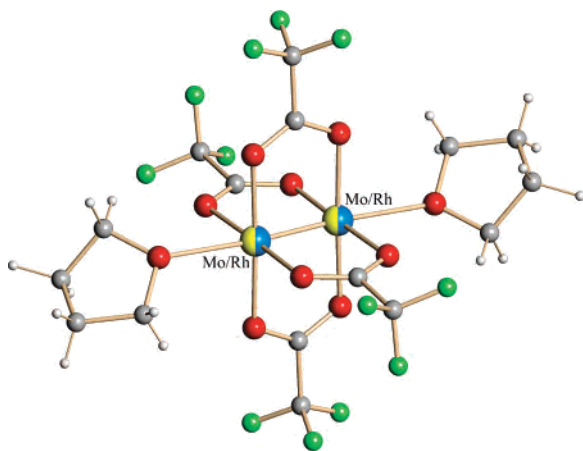


Figure 2. Molecular structure of the bis-adduct, $[(\text{MoRh})(\text{O}_2\text{CCF}_3)_4] \cdot (\text{THF})_2$ (**2**). Each metal position is refined as 50% Mo and 50% Rh.

this new complex was also found to be isomorphous to the corresponding homometallic bisadducts with only one crystallographically independent metal position in the crystal structure (Figure 2). Here again, the M–M and axial M···O distances fall between the corresponding distances for the THF bisadducts of the $[\text{Mo}_2]$ and $[\text{Rh}_2]$ molecules (Table 2). It is worth mentioning here that a similar picture has been observed for the bis-acetic acid adduct of the Cu–Rh acetate,¹¹ which, we believe, conforms to the structure type **B** with a statistical distribution of homodinuclear units.

The results of spectroscopic investigation of bimetallic carboxylate **1** suggest that it consists of homometallic units. Thus, the ^{19}F NMR spectrum features two signals corresponding to those of dirhodium and dimolybdenum tetra(trifluoroacetates) (Table 3). It should be noted that for a “true” heterometallic molecule, $[(\text{BiRh})(\text{O}_2\text{CCF}_3)_4]$, we observed⁹ a single peak in the fluorine NMR spectrum. The IR spectrum of **1** shows two strong peaks at 1593 and 1655 cm^{-1} for $\nu_{\text{asym}}(\text{CO})$ that are close to the corresponding peaks for dimolybdenum and dirhodium compounds, respectively. Finally, the UV–vis spectrum of **1** looks similar to the one obtained for the mixture of molybdenum(II) and rhodium(II) trifluoroacetates.

The convincing evidence that the bimetallic Mo/Rh carboxylate consists of homometallic dimolybdenum and dirhodium units has been obtained from a mass spectrometric investigation in the acetone solution and from magnetic measurements in the solid state. The negative TOF mass spectrum of **1** (Figure 3) shows peaks corresponding to homometallic $[\text{Mo}_2(\text{O}_2\text{CCF}_3)_5]^-$ and $[\text{Rh}_2(\text{O}_2\text{CCF}_3)_5]^-$ ions, which are in perfect match with the calculated isotope distribution patterns. Importantly, no peaks attributed to any heterometallic fragments were found in the spectrum because the isotope distribution pattern for heterometallic fragments should be significantly different from those for homometallic ions. Similarly, the magnetic susceptibility measurements on crystalline sample of **1** over the range of 60–300 K (see Supporting Information for more details) indicate diamagnetic properties of the bimetallic complex. If the molybdenum/rhodium trifluoroacetate was of the structure type **A**, that would result in the odd-electron d^4-d^7 configuration. However, the diamagnetic character of the compound is in a good agreement with the **B** type structure containing homometallic Mo_2 (d^4-d^4) and Rh_2 (d^7-d^7) units.

The bimetallic molybdenum/rhodium trifluoroacetate (**1**) reported here contains homometallic paddlewheel units that form polymeric chains through Lewis acid–base interactions in the solid-state structure. In solution, **1** dissociates to the $[\text{Mo}_2]$ and $[\text{Rh}_2]$ units that have solvent donor molecules coordinated to their axial positions. Thus, in solution, **1** is indistinguishable from the mixture of homometallic trifluoroacetates. However, in the solid state, the bimetallic compound is not simply a mixture of homometallic carboxylates and still provides some degree of homogenization at the molecular level. This is evident from the results of thermogravimetric analysis. While the TGA curve for the mixture of $[\text{Mo}_2(\text{O}_2\text{CCF}_3)_4]$ and $[\text{Rh}_2(\text{O}_2\text{CCF}_3)_4]$ shows a two-step decomposition pattern corresponding to thermal behavior of individual compounds (Figure 4), the thermal degradation of **1** is an essentially one-step process that starts at higher temperature and results in a distinctly different residue.

In a reference to the Scheme 1B, we tend to believe that there should be a statistical, rather than ordered, distribution

(11) Antsyshkina, A. S.; Mityrakina, M. A.; Yurchenko, E. N.; Gracheva, L. S. *Russ. J. Inorg. Chem.* **1991**, *36*, 1725.

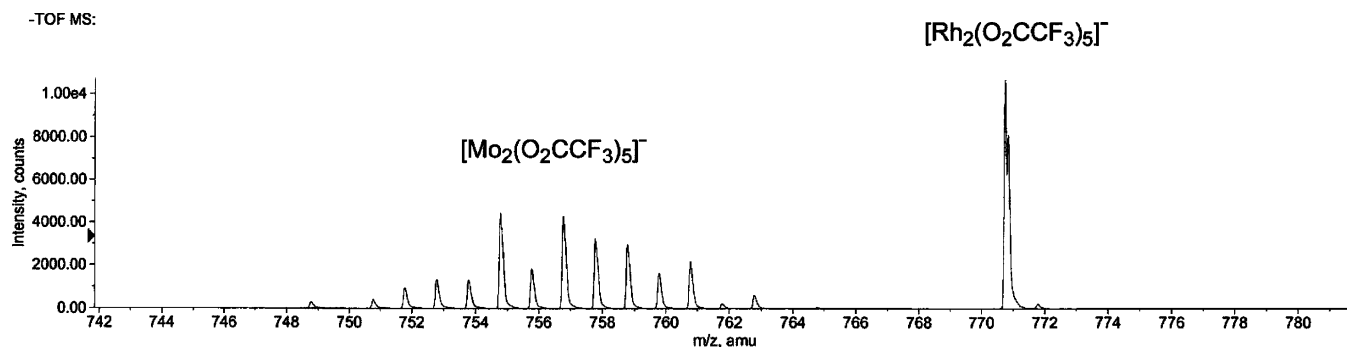


Figure 3. Negative ion TOF-MS mass spectrum of **1** in acetone.

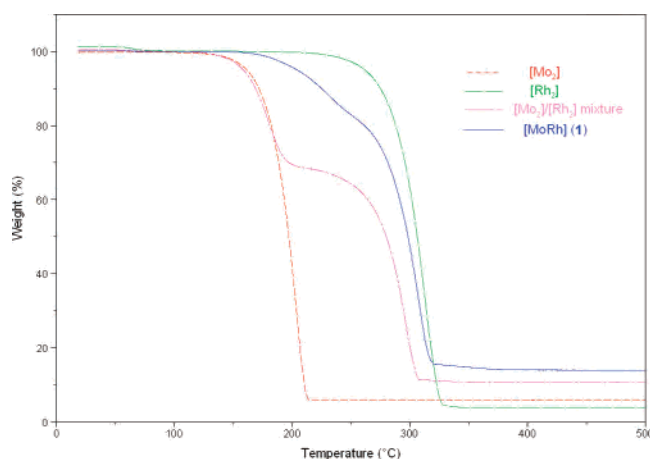


Figure 4. Thermogravimetric analyses of **1** compared with parent homometallic carboxylates and their physical mixture.

of homometallic dinuclear units in the crystal structure of **1**. That is based on observation that mixed-metal compounds with compositions different from that of Mo/Rh = 1:1 can be prepared. We were able to isolate at least one of such bimetallic carboxylates, for which elemental analysis gives a metal content of 70% Mo and 30% Rh. As expected, the unit cell dimensions, as well as the M–M (2.2152(3) Å) and M···O (2.523(3) Å) distances, in this structure are closer to those of molybdenum(II) trifluoroacetate.

The formation of the bimetallic compound **1** can be considered to be a result of isomorphous substitution.¹² The overall dimensions of the $[\text{Mo}_2(\text{O}_2\text{CCF}_3)_4]$ and $[\text{Rh}_2(\text{O}_2\text{CCF}_3)_4]$ units are very similar with the sole exception of the metal–metal bond length. However, when an aggregation of bimetallic units into infinite chains is considered, the addition of intermolecular axial M···O contacts to the M–M bonds is giving very close distances for a chain step, ~4.78 and 4.72 Å, respectively. In other words, the $[\text{Mo}_2]$ and $[\text{Rh}_2]$ blocks are commensurate in the solid-state structure providing a basis for isomorphous substitution. In agreement with this, we have failed to obtain any new mixed-metal Mo–Rh compounds by reaction with the corresponding pivalate and trifluoroacetate complexes that are known to have significantly different dimensions that primarily affect the interchange contacts.

Experimental Section

All of the manipulations were carried out in a dry, oxygen-free, dinitrogen or argon atmosphere employing standard ampule, glovebox, and Schlenk techniques. All chemicals, unless otherwise described, were purchased from Aldrich and used as received. All solvents used were anhydrous and kept under the protection of activated molecular sieves. The dirhodium(II) and dimolybdenum(II) tetra(trifluoroacetates) were prepared according to the literature procedures.^{10,13} Single crystals of $[\text{Mo}_2(\text{O}_2\text{CCF}_3)_4]$ were obtained by sublimation at 170 °C in a sealed, evacuated ampule. Crystals of bis-THF adducts for $[\text{Mo}_2(\text{O}_2\text{CCF}_3)_4]$ and $[\text{Rh}_2(\text{O}_2\text{CCF}_3)_4]$ were obtained from saturated THF solutions at –10 °C. UV–vis spectra were acquired using a Hewlett-Packard 8452A diode array spectrophotometer. IR spectra were recorded on a Nicolet Magna 550 FTIR spectrometer using KBr pellets. NMR spectra were obtained using a Bruker Avance 400 spectrometer at 376.47 MHz for ¹⁹F. Chemical shifts are reported in parts per million (ppm) relative to CFCl_3 . Electropray mass spectra were acquired on a MDS Sciex API QStar Pulsar mass spectrometer using an electropray ionization source. The spectra were acquired in the negative ion mode in an acetone solution of ~50 μM analyte concentration. The magnetic susceptibility measurements were performed with the use of a Quantum Design SQUID magnetometer MPMS-XL. The data were obtained on finely ground crystalline sample of **1** (23.1 mg) in an applied magnetic field of 0.1 T in the temperature range of 60–300 K. The magnetic data were corrected for the sample holder background. Elemental analyses were performed by Maxima Laboratories, Guelph, Canada.

[(MoRh)(O₂CCF₃)₄] (1). A mixture of $[\text{Rh}_2(\text{O}_2\text{CCF}_3)_4]$ (0.20 g, 0.30 mmol) and $[\text{Mo}_2(\text{O}_2\text{CCF}_3)_4]$ (0.064 g, 0.10 mmol) was sealed in an evacuated glass ampule and placed in an electric furnace having a temperature gradient (~5 °C) along the length of the tube. The ampule was kept at 150 °C for 7 days to allow greenish crystals of **1** to be deposited in the cold section of the container. The yield was ~70% (crystals collected). ¹⁹F NMR (C_7D_8 , 22 °C): δ –71.497 (s, CF_3), –73.948 (s, CF_3). IR (KBr, cm^{-1}): 1655s, 1593s, 1458 m, 1238sh, 1192s, 1156sh, 860 m, 782 m, 740s, 528 m. UV–vis (C_7D_8 , 22 °C) λ_{max} , nm (ε, $\text{M}^{-1} \text{cm}^{-1}$): 310 (6621), 352 (5803). –TOF MS (CHCl_3 , m/z): 1400.58 ($[\text{Mo}_4(\text{O}_2\text{CCF}_3)_9]^-$), 863.20 ($[\text{Rh}_2(\text{O}_2\text{CCF}_3)_5(\text{O}_2\text{CCF}_2)]^-$), 770.80 ($[\text{Rh}_2(\text{O}_2\text{CCF}_3)_5]^-$), 754.79 ($[\text{Mo}_2(\text{O}_2\text{CCF}_3)_5]^-$), 702.79 ($[\text{Mo}_2(\text{O}_2\text{CCF}_3)_4(\text{C}_2\text{OF})]^-$), 688.79 ($[\text{Mo}_2(\text{O}_2\text{CCF}_3)_4(\text{CO}_2)]^-$). Anal. Calcd for $\text{C}_8\text{O}_8\text{F}_{12}\text{MoRh}$: Mo 14.74%, Rh 15.81%. Found: Mo 14.27%, Rh 14.78%.

[(MoRh)(O₂CCF₃)₄](THF)₂ (2). Crystals of $[(\text{MoRh})(\text{O}_2\text{CCF}_3)_4]$ (**1**) (0.050 g) were dissolved in THF (1.0 mL) inside an NMR tube to afford a greenish solution. Hexane (3.0 mL) was then added carefully using a syringe on top of the THF layer. The tube was

(12) (a) Kessler, V. G. *Chem. Commun.* **2003**, 1213. (b) Sulikowski, B. *Heterog. Chem. Rev.* **1996**, *3*, 203.

(13) Cotton, F. A.; Norman, J. G., Jr. *J. Coord. Chem.* **1972**, *1*, 161.

Table 4. Crystallographic Data and Structure Refinement Parameters

	1	2	[Mo ₂]	[Mo ₂](THF) ₂	[Rh ₂](THF) ₂
formula	MoRhO ₈ C ₈ F ₁₂	MoRhO ₁₀ C ₁₆ H ₁₆ F ₁₂	Mo ₂ O ₈ C ₈ F ₁₂	Mo ₂ O ₁₀ C ₁₆ H ₁₆ F ₁₂	Rh ₂ O ₁₀ C ₁₆ H ₁₆ F ₁₂
fw	650.93	795.14	643.96	788.17	802.11
cryst syst	triclinic	triclinic	triclinic	triclinic	triclinic
space group	<i>P</i> $\bar{1}$	<i>P</i> $\bar{1}$	<i>P</i> $\bar{1}$	<i>P</i> $\bar{1}$	<i>P</i> $\bar{1}$
<i>a</i> (Å)	5.3385(5)	8.7543(6)	5.5662(8)	8.7817(7)	8.5503(8)
<i>b</i> (Å)	8.4547(8)	9.0902(6)	8.2207(12)	9.0928(7)	9.1936(9)
<i>c</i> (Å)	9.1418(8)	9.4058(6)	8.9579(13)	9.4597(7)	9.4802(9)
α (deg)	89.6540(10)	63.1370(10)	87.515(2)	62.7350(10)	63.5900(10)
β (deg)	89.6720(10)	78.3180(10)	85.862(2)	78.2750(10)	77.0350(10)
γ (deg)	77.0450(10)	77.8010(10)	80.617(2)	77.4510(10)	76.5830(10)
<i>V</i> (Å ³)	402.11(6)	647.72(7)	403.15(10)	650.70(9)	642.92(11)
<i>Z</i>	1	1	1	1	1
ρ_{calcd} (g cm ⁻³)	2.688	2.038	2.652	2.011	2.072
μ (mm ⁻¹)	1.980	1.255	1.729	1.097	1.418
transm factors	0.6929–0.9250	0.8439–0.9063	0.3995–0.8471	0.7135–0.8441	0.7945–0.9197
temp (K)	173(2)	173(2)	173(2)	173(2)	173(2)
data/restraints/params	1790/18/146	2925/36/232	1768/0/137	2893/36/231	2851/36/199
R1, ^a wR2 ^b					
<i>I</i> > 2 σ (<i>I</i>)	0.0301, 0.0766	0.0388, 0.1049	0.0220, 0.0574	0.0373, 0.0984	0.0467, 0.1164
all data	0.0305, 0.0769	0.0399, 0.1038	0.0222, 0.0576	0.0380, 0.0994	0.0597, 0.1244
GOF ^c	1.081	1.050	1.050	1.047	1.014

^a $R1 = \sum ||F_o| - |F_c|| / \sum |F_o|$. ^b $wR2 = [\sum [w(F_o^2 - F_c^2)^2] / \sum [w(F_o^2)^2]]^{1/2}$. ^c $GOF = [\sum [w(F_o^2 - F_c^2)^2] / (N_{\text{obsd}} - N_{\text{params}})]^{1/2}$, based on all data.

kept in a freezer at -20 °C for one week to allow pale-violet crystals of **2** to be deposited at the bottom.

In an alternative approach, crystals of [(MoRh)(O₂CCF₃)₄] (**1**) (0.050 g) were dissolved in THF, and the solvent was then gently evaporated. The solid residue was sealed in an evacuated glass ampule and placed in an electric furnace having a temperature gradient (~ 5 °C) along the length of the tube. The ampule was kept at 100 °C for 3 days to allow pale-violet crystals of **2** to be deposited in the cold section of the container.

X-ray Crystallographic Procedures. Selected single crystals suitable for X-ray crystallographic analysis were used for structural determination. The X-ray intensity data were measured at 173(2) K (Bruker KRYOFLEX) on a Bruker SMART APEX CCD-based X-ray diffractometer system equipped with a Mo-target X-ray tube ($\lambda = 0.71073$ Å) operated at 1800 W power. The crystals were mounted on a goniometer head with silicone grease. The detector was placed at a distance of 6.140 cm from the crystal. For each experiment, a total of 1850 frames were collected with a scan width of 0.3° in ω and an exposure time of 20 s/frame. The frames were integrated with the Bruker SAINT Software package¹⁴ using a narrow-frame integration algorithm to a maximum 2θ angle of 56.54° (0.75 Å resolution). The final cell constants are based upon the refinement of the XYZ-centroids of several thousand reflections above $20\sigma(I)$. Analysis of the data showed negligible decay during data collection. Data were corrected for absorption effects using the empirical method (SADABS). The structures were solved and refined by full-matrix least-squares procedures on $|F^2|$ using the

Bruker SHELXTL (version 6.12) software package.¹⁵ The coordinates of metal atoms for the structures were found in direct method *E* maps. The remaining atoms were located after an alternative series of least-squares cycles and difference Fourier maps. For **2** and the bis-THF adduct of [Mo₂(O₂CCF₃)₄], the hydrogen atoms were located and refined independently; for the bis-THF adduct of [Rh₂(O₂CCF₃)₄], hydrogen atoms were included in idealized positions for structure factor calculations. The fluorine atoms of some CF₃ groups appeared to be disordered over three rotational orientations. Anisotropic displacement parameters were assigned to all non-hydrogen atoms, except the disordered fluorine atoms. Relevant crystallographic data are summarized in Table 4.

Acknowledgment. This work is dedicated to the memory of Professor F. Albert Cotton. Acknowledgment is made to the Donors of the American Chemical Society Petroleum Research Fund, Grant 44770-AC3, for support of this work. We also thank the National Science Foundation, Grant NSF-0619422 (X-ray diffractometer).

Supporting Information Available: Magnetic measurements data, –TOF-MS, NMR, IR, and UV–vis spectra, and X-ray crystallographic files in CIF format. This material is available free of charge via the Internet at <http://pubs.acs.org>.

IC7009012

(14) SAINT, Data Reduction Software, version 6.22; Bruker Analytical X-ray Systems, Inc.: Madison, WI, 2001.

(15) Sheldrick, G. M. SHELXTL, version 6.12; Bruker Analytical X-ray Systems, Inc.: Madison, WI, 2000.